System level modeling of MEMS at TU Chemnitz MEMS-Design group

Vladimir A. Kolchuzhin, Jan E.Mehner

Technische Universität Chemnitz, Fakultät für Elektrotechnik und Informationstechnik,
Professur für Mikrosystem- und Gerätetechnik
Chemnitz, Germany

Summary

The paper is focused on system level modeling of MEMS using advanced reduced order modeling (ROM) methods based on mode superposition technique and finite element solvers for data extraction. Dynamically accurate behavior representations can be achieved for microstructures with flexible components and their most important interactions with thermal, electrostatic, magnetic and fluid fields. The results are macromodels based on analytical terms which can be transferred to electronic and system simulators for virtual prototyping and device analyses. To demonstrate the theory of the proposed methods and its possibilities, few examples are presented: vibration parameterized electrostatically actuated fixed-fixed beam and SWCNT-based mechanical sensor.

Keywords

system level modeling, MEMS, reduced order modeling, parametric modeling

1. Introduction

Microelectromechanical systems, actuated by electrostatic force are widely used in various applications such as the inertial sensors (accelerometers, gyroscopes, vibration and AE-sensors), RF-components (switches, resonators, filters and tunable capacitors), micromirrors, microphones, pressure sensors, magnetometers, and test stage for nanosystems. The NEMS/MEMS designing is a very challenging multilevel and interdisciplinary task. The levels in design include synthesis of lumped elements, process sequence development and mask layout drawing, component and system simulations. Different algorithms and software tools are used for this purpose. Numerical simulations are used both as a design tool and for understanding complex device behavior. Commonly used numerical simulation methods (FDM, FEM and BEM) provide results for a given set of geometrical and material parameters.

Activities of the MEMS-Design group at the Chemnitz University of Technology are focused on metrology development for device and system simulation levels, on modeling and simulation of user-specific applications and practical MEMS design for prototypes manufactured. Beyond the commercial software the paper deals with advanced computational approaches required to extend the considered effects at system level. The presentation gives a short overview of the approaches developed at TU Chemnitz over the past decade [1-14] and is subdivided into five chapters. As part of the outline, the ANSYS ROM Tool (ANSYS Mechanical APDL) which implements the generation of MEMS system model is summarized in Chapter 2. Parameterization of models is highlighted in Chapter 3: the parametric modeling based on mesh morphing and parametric discrete analysis are illustrated by examples. In Chapter 4 the mechanical contact phenomena at system level is described. Chapter 5 presents a description of CNT based mechanical sensor, single walled CNT compact model implementation using hardware description languages and co-simulation with MEMS test stage.

2. Reduced order modeling methods based on mode superposition technique

Nowadays, the mode superposition method (MSM) has become the industry standard for macromodels extracting of MEMS with flexible components [15-20]. The MEMS suppliers like IC ones can provide model libraries for their electro-mechanical components. The ROM macromodels are generated by numerical data sampling and subsequent fit algorithms. Starting from a full order finite element model with structural, electrostatic and thin film fluid elements, an automated ROM generation must be performed in order to create database information. The MSM based ROM model has a good scalability at system level. A schematic view on the generalized ROM layout and interfaces of typical electro-mechanical system is shown in Figure 1.

The strain energy, the mutual capacitances, the damping coefficients and the modal load forces are the parameters characterizing the coupled electro-mechanical system [21]. The ROM macromodels capture the complex nonlinear dynamics inherent in MEMS due to highly nonlinear electrostatic forces, residual stresses, stress stiffening and supports multiple electrode systems and mechanical contact phenomena at system level. The entity transducer element (the ROM144 functional block in Figure 1) describes the interface of macromodel. Each DOF of the ROM element is mapped to one of the across or through quantities of the terminals of the entity. At the modal terminals the modal amplitude q_i and external modal force fm_i (e.g. acceleration, angular rate) are available for the chosen modes. The master node terminals provide the displacement u_i and the inserted forces fn_i at these nodes. At the electrical terminals the voltages V_j and currents I_j are available for the electrodes of the system.

Using modal projection method presented in [22], the ROM model is able to capture nonlinear squeeze film phenomena (ROM140 functional block), such as deflection dependent damping and stiffening.

The ROM method based on mode superposition method is very effective technique for fast transient simulation of MEMS component. Efficiency of reduced order models becomes obvious if one considers the total number of differential equations to be solved. There is only one equation for each eigenmodes (basis function) and one equation for each conductor [1, 22]. The extracted macromodel can be automatically export to most common simulation tools at system level as signal flow graphs system Simulink, PSPICE circuit simulators and VHDL-AMS, VERILOG-AMS simulators.

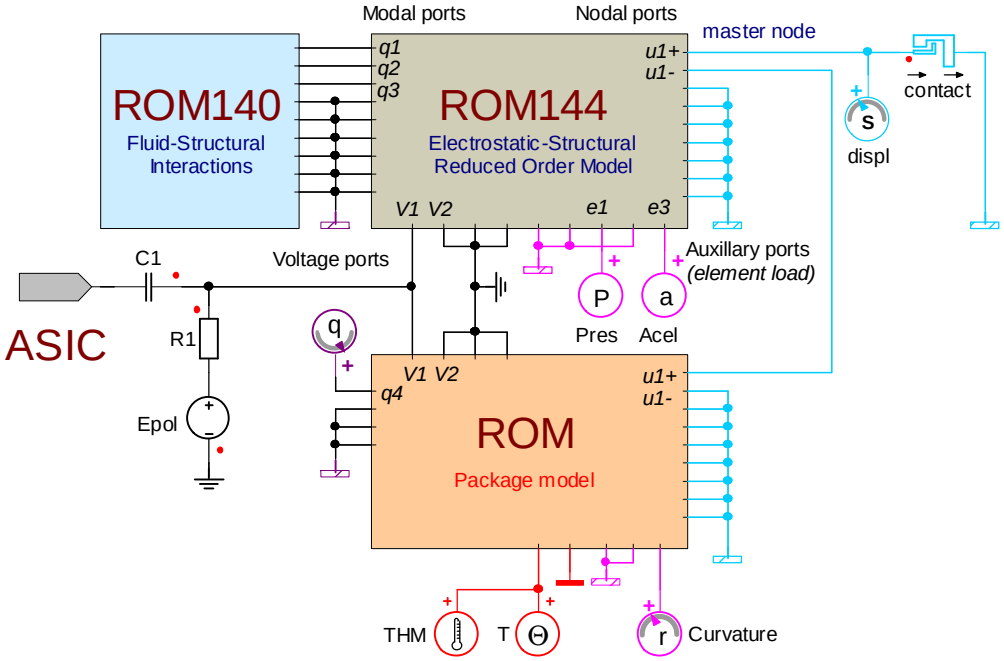

Fig. 1. A schematic view on the VHDL-AMS exported ROM model in Simplorer

3. Parametric modeling

Drawback of the existing ROM techniques is that those algorithms can only analyze a single model configuration with specified dimensions and physical parameters. In practice, there is necessity to know the influence of parameter variations on the structural response in order to optimize the entire system and to assess the effect of technology tolerances or changed material. Traditional, parametric model is extracted by series of finite element simulations and subsequent function fit procedures (multivariate polynomial/rational fitting, multivariate splines, multidimensional Gaussian process regression) Recently, parametric ROM using data sampling approach and design optimization algorithms has been presented to the angular rate sensor [23].
Alternatively to the data sampling techniques, power expansion approach for behavioral model extraction and building response surfaces was investigated in [9-10]. Like polynomial fitting, the power expansion is also using a polynomial form for the response surface, but the polynomial represents a Taylor expansion at the initial point of the variation range of the parameters. Padé approximants can be used to transform of a Taylor series into a rational function, e.g. ANSYS *Variational Technology* is a tool to provide accurate, high-order response surfaces based on a *single* finite element analysis [10]. The key idea of the parametric approach is to compute not only the governing system matrices of the corresponding FE problem but also high order partial derivatives (HOD) with regard to design parameters by means of the automatic differentiation [7]. Reusing of the factorized **M**, **K** matrices and its derivatives at the initial point for different type of analyses can increase the efficiency of the method. In particular, the time consuming data sampling process in the static and frequency response domains has been replaced by a set of single FE runs on the basis of the structural, electrostatic and squeeze film analyses with regard to selected design parameters.

3.1 Parametric modeling based on mesh morphing

The comb-drive consisting of interdigitated fingers is one of the main component of MEMS resonators. The parametric model extraction of the capacitive cell using one FE solution is presented as an application of the general HOD methodology. Three geometrical parameters (side-wall angle α and shifts in *x* and *y*-direction) are used to parameterize the model.
The perturbation of internal nodes with respect to shifts in *x* and *y*-direction is obtained by solving Laplace's equation with Dirichlet boundary conditions. The initial mesh (α=0 and shifts u_x=0 and u_y=0) and contour plot of design velocity for perturbation of internal nodes are shown in Figure 2a. The perturbated meshes with regard to the α and u_y are visualized in Figures 2b-2c respectively.

Figure 3 illustrate the capacitance relationship depending on design parameters. It is essential that the response functions not only provide the capacitance data but also the first and second derivatives needed for Maxwell force and electrostatic softening computations. The obvious disadvantage is that applicable range limited by mesh-morphing procedures. The large mesh perturbation of electrostatic FE mesh is a bottleneck and cannot be applied in parametric analysis [7].

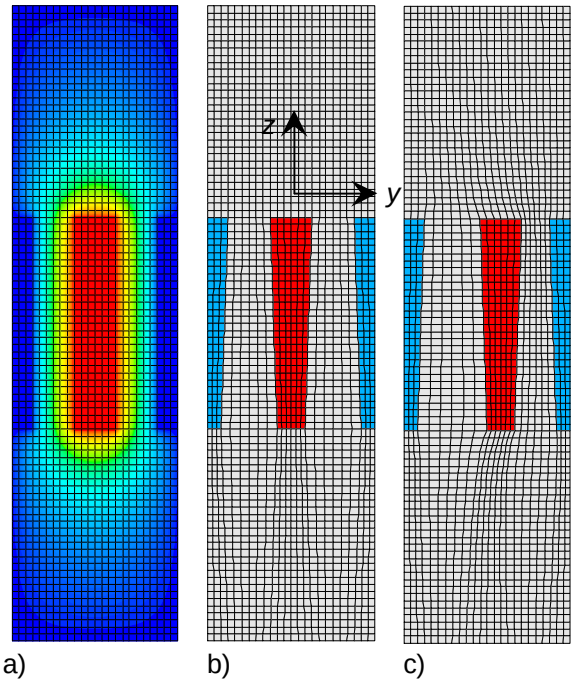

Fig. 2. Mesh-morphing for parametric modeling a) initial mesh and contour plot of design velocity $v(x,y,z)\in[0...1]$ for mesh perturbations; b) mesh perturbation with a=1.0°; c) mesh perturbation with a=1.0° and u_y=1.0μm;

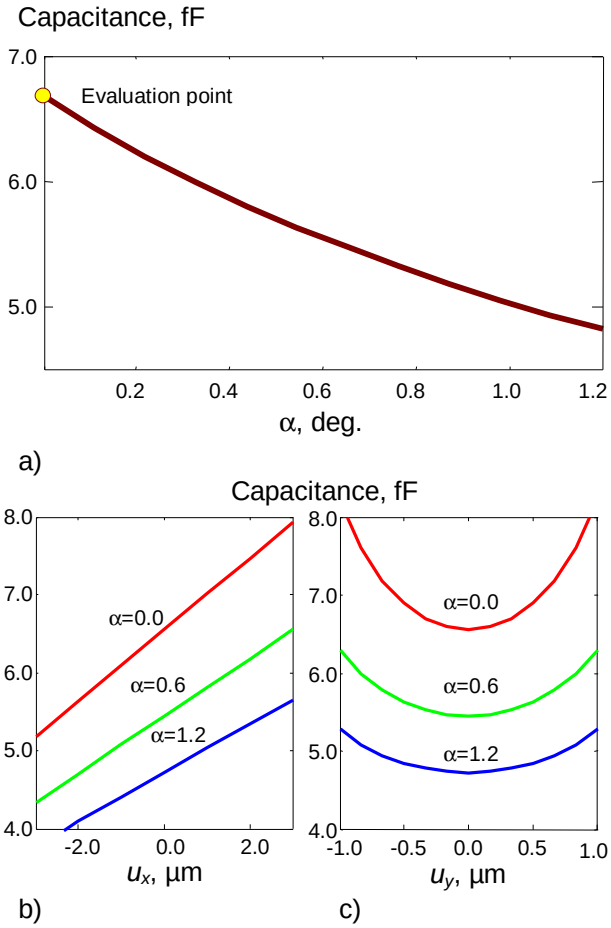

Fig. 3. Extracted at the one evaluation point capacitance with regard to side-wall angle

3.2 Parametric discrete analysis

The aim of this section is to illustrate how the high order derivatives analysis can be used in the discrete analysis. The groups of elements (components) can be considering as discrete parameters or Boolean parameters. Typical examples of such features would be ribs or holes. The effects of removing these components from the model can be study by changing their material properties. Discrete parameter corresponds to sets of elements in the model that can be turned **1** or **0**. Then **p** = **0**, the elements components remain in the model but contribute a near-zero stiffness (or conductivity, permittivity etc.) value to the global matrix like deactivates the specified element with the birth and death capability: $Y(p)=Y(0)\cdot p$.

The following example builds a perforated beam with circular holes having a radius of 10 μm. The perforations are widely used in MEMS for several reasons. The main purpose is to decrease the damping and spring forces of vibrating structures due to the gas flow in small air gaps. The second goal is to increase eigenfrequency due to reduce the total mass of structures. The five holes are set as discrete variables, allowing simulating the effects caused by removing holes. For *n* discrete parameters, the 2^n configurations can be explored at one solution step. The five holes are group into three element components as shown in Figure 4.

For the present study, the 8 configurations have been explored. The initial point **p** = {1,1,1} was used for extracting the derivatives of solution vector. Exemplarily, the obtained parametric solution is illustrated for static structural analysis in Figure 5. The result demonstrates that the displacement could be captured correctly by the polynomial of degree 5. Taylor series converge slowly, because the

evaluation and estimated points are located at the ends of interval. Numerical tests have shown that in case of the distributed loads (e.g. pressure) also needs to correct the load for removing area. Then $p_i \rightarrow 0$, the surface load applied to the *i*-element component must have zero contributes in order to extract a correct parametric solution.

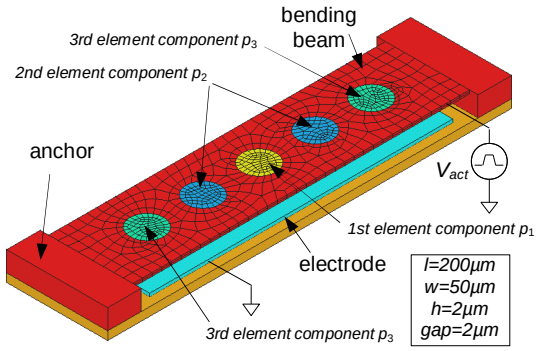

Fig. 4 FE-model of a perforated beam

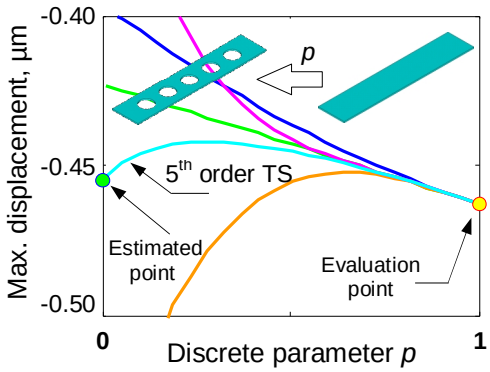

Fig. 5 Results of a discrete static analysis of a perforated beam under electrostatic pressure

The histogram in Figure 6 visualizes obtained results in the static, modal, frequency response domains on the basis of the structural, electrostatic and coupled field analyses. All units are normalized to the maximal values in terms of relative values. Different optimization methods such as Monte-Carlo or genetic algorithms can be used to determine the best configuration using extracted parametric database.

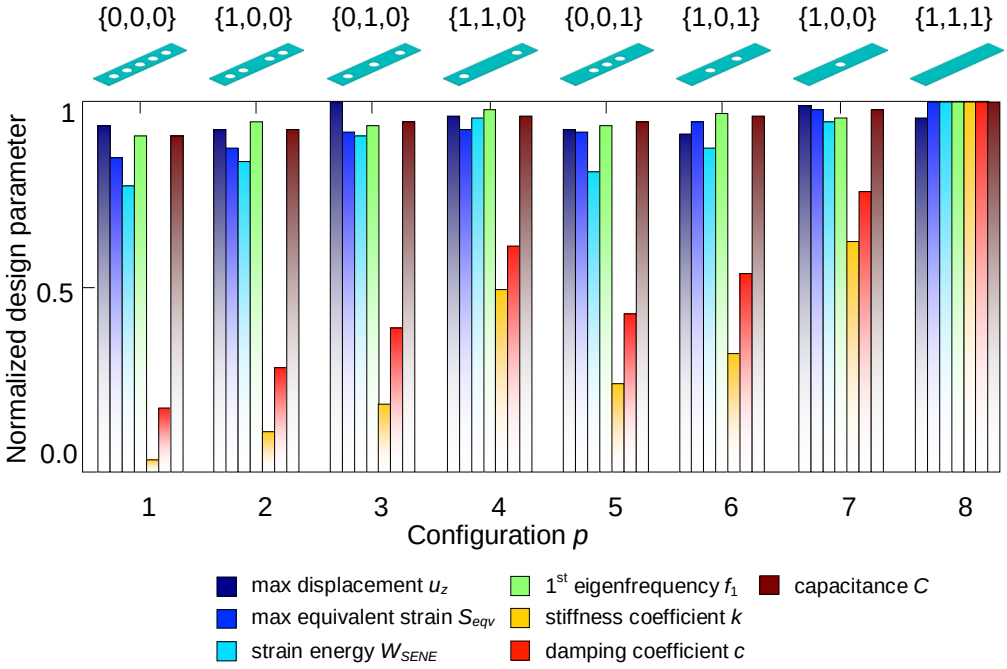

Fig. 6 Discrete analyses results of a perforated beam

4. Mechanical contact phenomena at system level

The expansion of the mode superposition approach to capture the strongly nonlinear mechanical contact behavior of MEMS including surface interactions is still a major challenge although huge progress has been made [1, 2, 15, 24]. One basic approach of modeling contacts without surface interactions has been presented by F. Bennini [1]. It has been shown that structural deformations due to contact can be represented by superposition of a sufficient large number of mode shapes. Unfortunately, the memory and computational costs of the process grow exponentially with the number of the modes. This paper presents an extended approach including surface interactions of

stiction and gap dependent squeeze damping. The governing equations of motion within modal space can be distinguished between noncontact and contact case. For the first case of noncontact the equations are given by

$$\ddot{q}_i + 2x_i w_i \dot{q}_i + w_i^2 q_i = f_i^{ext} + f_i^{\mathrm{T}} \mathbf{F}_D(u) \tag{1}$$

where q_i are the modal amplitudes, ω_i are the eigenfrequencies, x_i are the modal damping ratios, f_i^{T} are the basis functions and f_{ext} are the external modal loads. The term $\mathbf{F}_D(u)$ corresponds to the gap dependent squeeze damping force vector in Equation 1. It is required in case of large deflections when plane components get close to each other and the arising nonlinear damping forces cannot be represented by constant modal damping ratios. However, modal damping ratios x_i should find consideration too, as squeeze damping is usually limited to a certain operating direction may causing undamped modes which are not affected by $\mathbf{F}_D(u)$.

An analytical solution for the squeeze damping force $\mathbf{F}_D^j(u)$ at master node *j* for perpendicular moving plates has been derived in [25] for small velocities from the simplified approach of the linearized Reynolds equations which assumes small displacements *u* and small gaps compared to plate dimensions.

$$F_D^j(u) = \frac{3 I_t h_{eff} \dot{u}}{(gap - u)^3} \tag{2}$$

I_t corresponds to the torsional stiffness of a beam cross section, gap to the initial separation between both plates and h_{eff} to the effective viscosity. Although this solution was derived under assumption of small displacements own simulations indicated the validity of the linearized Reynolds equation even for large displacements which has also been reported by Turowski et al. [26]. Equation (2) has been modified into

$$F_D^j(u) = \begin{cases} 0, & if\ u \le u_s \\ \dfrac{3 I_t h_{eff} \dot{u}}{(gap - u)^3} - \dfrac{3 I_t h_{eff} \dot{u}}{(gap - u_s)^3}, & if\ u > u_s \end{cases} \tag{3}$$

in order to account for nonlinear squeeze damping from a chosen deflection level u_s. Equation (3) includes a term of rectification in order to avoid over damping into gap direction *u* due to superposition of modal and local damping. In terms of contact the system equation of motion is given by

$$\ddot{q}_i + 2x_i w_i \dot{q}_i + w_i^2 q_i = f_i^{ext} + f_i^{\mathrm{T}} \left(\mathbf{F}_D^j(u) + \mathbf{F}_C^j(u) \right),$$

where $\mathbf{F}_C^j(u)$ corresponds to the contact force vector at master node *j* which can be distinguished in a compressive part $\mathbf{F}_{C-com}^j(u)$ and in an adhesion part $\mathbf{F}_{C-adh}^j(u)$:

$$F_C^j(u) = \begin{cases} F_{C-com}^j, & if\ F_C^j > 0 \\ F_{C-adh}^j, & if\ F_C^j < 0 \end{cases}.$$

The developed model has been used to identify acting adhesion forces based on the measured pull-out behavior [27 ,28]. Figure 7 illustrated an example of beamlike tests structures intended to investigate sticking effects to side walls where stops of different contact size are near the beam tips. The beams are brought into contact with their stops by applying an actuation voltage to the electrodes. After the contact is reached the voltage is set to ground and the shortest adhering beam gives a rough estimation on acting sticking forces. A more precise determination is given by using pull-out voltage in order to calculate acting sticking forces. The Polytec MSA-500 in-plane motion analyzer enables an optical detection of pull-out voltages.

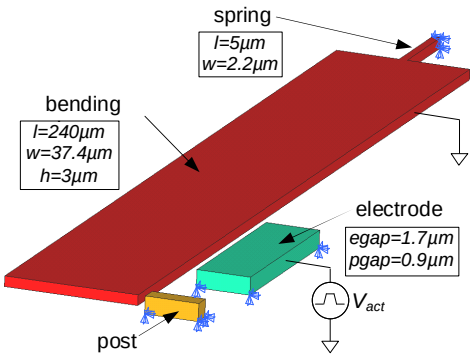

Fig. 7 Bending beam for sticking investigations

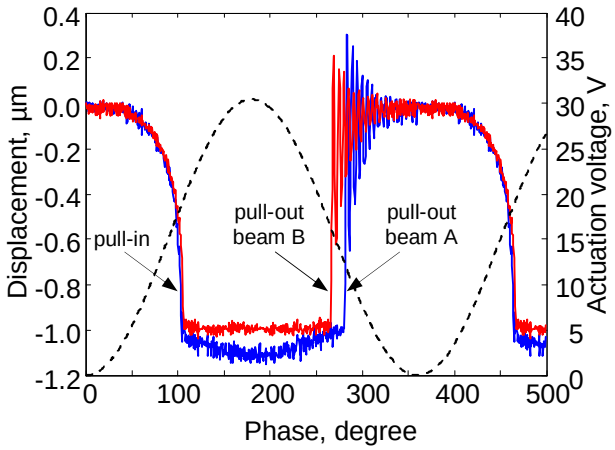

Fig. 8 Measured contact behavior

Figure 8 shows the displacement of two equal beams with different stop size near their tips. A sinusoidal voltage of low frequency and with a DC offset has been used in order to bring the structures into contact with the stops. After the maximum voltage is reached it decreased until pull-out occurs. Due to the different sizes of the used stops, pull-out voltage differ of about 3.5 V which means varying sticking forces between both beams. A numerical model has been used to calculate acting sticking forces from determined pullout voltages.
From the results [27] it becomes obvious that there is only a very small dependency of sticking forces on contact size since the nature of contact is punctual due to the large surface roughness. Large stop sizes lead to a reduction of sticking forces due to an increasing peel off behavior for large contact length.
The impact model can be used to identify design parameters of flexible stops which are applied to limit arising impact forces and, hence, increase the reliability of movable microstructures [29, 30].

5. Integration of MEMS/NEMS models at the system level

The nano-scale is explored to look out for new sensing principles and one of them is the piezoresistive effect of carbon nanotubes, useful for a nano-scaled acceleration sensor. Recently, several groups have reported on techniques for making networks of CNTs that can be placed onto metallic pads [31].

5.1. Design concept of the SWCNT based mechanical sensor

The virtual prototype of CNT based mechanical sensor consists of MEMS test stage that is served to actuate single-axis force. The single CNT is placed between the movable and fixed electrodes. The change in conductivity of CNT, when strain is applied, is used to measure force and displacement. A schematic view on the sensor layout and interfaces is shown in Figure 9. It should be noted, that gauge factor of CNT decreases as the chiral angle increases and the zigzag tubes (*n*,0) have a maximum magnitude of gauge factor [31].
The length L_{CNT} of the tube is defined by minimal available air gap between the movable and fixed electrodes (2µm in BDRIE process). In order to avoid damaging the CNT, a measurement is limited in the relative deformation range of 0 to +5 %. The electrostatic comb drive is used to set the operating point (OP) on the strain-displacement curve of CNT.

5.2. Implementation in VHDL-AMS

The SWCNT at the system level is presented as a four terminals device (two mechanical and two electrical terminals), which consist of the nonlinear mechanical spring unidirectional coupled with the strain dependent resistor. The behavioral model of spring is defined by:

$$f(t) = k_{\mathrm{CNT}} u(t) \qquad \text{in linear case and}$$

$$f(t) = \frac{\partial E_{tot}}{\partial u} \qquad \text{in nonlinear case,}$$

where CNT axial stiffness k_{CNT} can be given as:

$$k_{CNT} = A \cdot E / L_{CNT}(0) .$$

The Van-der-Waals distance (6.3 Å) is the distance of two neighbouring carbon sheets in graphite and can be used to define the effective cross section area *A*. For more details see [14].
The next step is to define the behavioral model of the resistor:

$$i(t) = v(t) / R_{CNT}(e) ,$$

where $e = u(t) / L_{CNT}(0)$ and the change in electrical resistance of ideal SWCNT due to mechanical strain e can be calculated by an empirical transport formula based on band-gap changes:

$$R_{CNT} = R_C + \frac{1}{|t|^2} \frac{h}{8e^2} \left[1 + \exp\left(\frac{E_{gap}(e)}{kT} \right) \right] .$$

Here, R_C denotes the contact resistivity; t^2 is the transmission probability of the nanotube, usually taken as 1; *h*, *e* and *k* are physical constants; *T* denotes the temperature and E_{gap} is the bandgap of the nanotube. The bandgap of a strained CNT is linearly changing with the relative deformation. An analytical formula for CNTs with a large radius is given in [14].

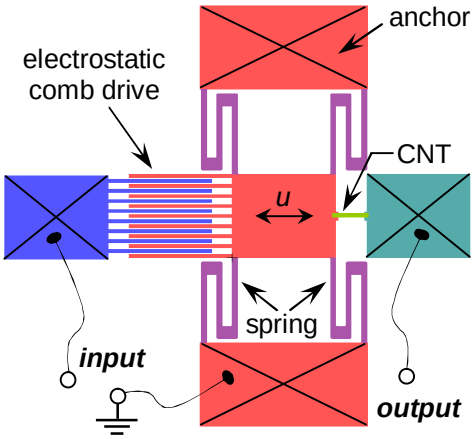

Fig. 9 The 2D layout of mechanical sensor

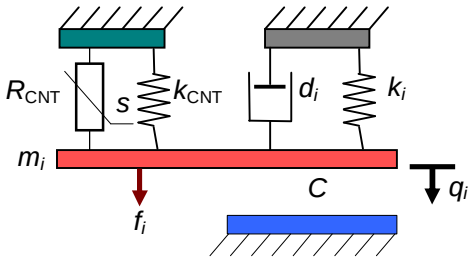

Fig. 10 Equivalent circuit model of CNT based sensor

The created macromodel of the MEMS test stage based on mode superposition technique was integrated in a testbench of the complete sensor for verification, Figure 10. The results of an analysis are shown below:

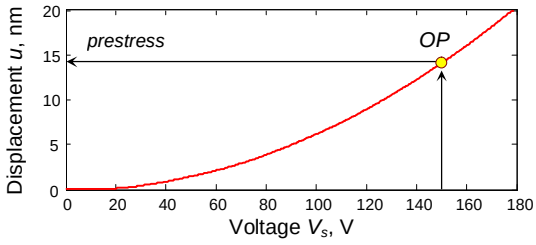

Fig. 11 Voltage-to-displacement curve of the MEMS test stage

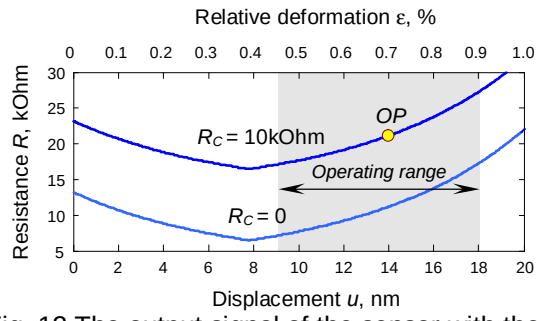

Fig. 12 The output signal of the sensor with the CNT (15,0)

A typical rectangular shaped comb drive design has a parabolic voltage-to-displacement relationship, which is a function of the change in electro-static force. The sensor is able to measure a displacement with nm resolution over a 10 nm range, Figure 12. Beyond this simple test case, one can analyse the SWCNT based mechanical sensor together with any other system environment or complex electronic circuit; perform the dimensioning design and parameters identification.

6. Conclusions

Advanced approaches to system level modeling for modeling and simulation of heterogeneous MEMS have been presented. The approaches are based on mode superposition method and the concept of generalized Kirchhoffian networks for multi-physical model allow generate parametric model libraries for NEMS/MEMS components. Parts of the presented work were carried out within the Collaborative Research Center SFB 379 "Arrays of micromechanical sensors and actuators" and the Research Unit 1713 "Sensoric Micro- and Nanosystems" which are funded by the German Research Association (DFG). The implemented theoretical approaches and developed benchmarks present the collaboration work of many colleagues at our Faculty. We would like to acknowledge the work of Michael Naumann and Dr. Erik Market.

7. References

[1] Bennini F., Mehner J., Dötzel W.: “System Level Simulations of MEMS Based on Reduced Order Finite Element Models”, Int. Journal of Computational Eng. Science, Vol. 2, No. 2, 2003, pp. 385-388

[2] Schlegel M., Bennini F., Mehner J., Herrmann G., Mueller D., Dötzel W., “Analyzing and Simulation of MEMS in VHDL-AMS Based on Reduced Order FE Models”, IEEE Sensors Journal, Vol. 5, No. 5, 2005, pp. 1019-1026

[3] Ansorge E.: “Untersuchungen zur Ordnungsreduktion magnetischer Systeme für dynamische Berechnungen“, Diplomarbeit, Technische Universität Chemnitz, 2003

[4] Bennini F.: “Ordnungsreduktion von elektrostatisch-mechanischen Finite Elemente Modellen für die Mikrosystemtechnik“, Dissertation, Technische Universität Chemnitz, 2005

[5] Gugel D.: “Ordnungsreduktion in der Mikrosystemtechnik“, Dissertation, Technische Universität Chemnitz, 2009

[6] Mehner J., Kolchuzhin V., Schmadlak I., Hauck T., Li G., Lin D. and Miller T.: “The influence of packaging technologies on the performance of inertial MEMS sensors”, Proc. of Transducers 2009, Denver, CO, Jun. 2009, pp. 1885-1888

[7] Kolchuzhin V.: “Methods and Tools for Parametric Modeling and Simulation of Microsystems based on Finite Element Methods and Order Reduction Technologies“, Dissertation, Technische Universität Chemnitz, 2010

[8] Markert E., Dienel M., Herrmann G., Heinkel U.: “SystemC-AMS assisted design of an Inertial Navigation System“, IEEE Sensors Journal, Vol. 7, Issue 5, 2007, pp. 770-777

[9] Kolchuzhin V., Mehner J., Gessner T., Dötzel W.: “Application of Higher Order Derivatives Method to Parametric Simulation of MEMS“, Proc. of EuroSimE, 2007, pp. 588-593

[10] Kolchuzhin V., Dötzel W., Mehner J.: “A Derivatives based Method for Parameterization of MEMS Reduced Order Models”, Proc. of EuroSimE, 2008, pp. 519-523

[11] Kolchuzhin V., Dötzel W., Mehner J.: “Challenges in MEMS parametric macro-modeling based on mode superposition technique”, Proc. of EuroSimE, Apr. 2009, pp. 442-445

[12] Kolchuzhin V., Naumann M., Mehner J.: “Recent developments in reduced order modeling based on mode superposition technique“, Proc. of EuroSimE, 2011, pp. 1-6

[13] Kolchuzhin V., Mehner, J.: “A parametric multilevel MEMS simulation methodology using finite element method and mesh morphing“, Proc. of EuroSimE, 2012, pp. 1-5

[14] Kolchuzhin V., Mehner J., Shende M.A., Markert E., Heinkel U., Wagner C., Gessner T.: “System level modelling of CNT based mechanical sensor“, 11. Chemnitzer Fachtagung Mikrosystemtechnik, Chemnitz, 2012

[15] Schauwecker B., Strohm K.A., Simon W., Mehner J., Luy J.-F.: “Toggle-Switch - A new type of RF MEMS switch for power applications”, IEEE MTT-S International Microwave Symposium Digest, 2002, pp. 219-222

[16] Döring C., Reitz S., Bastian J., Maute M., Schneider P., Schwarz, P.: “Verhaltens-modellierung eines Drehratensensors mittels Verfahren der Ordnungsreduktion”, Proc. of 10. GMM-Workshop, 2004

[17] Hauck T., Thanner M., O'Brien G.: “Dynamic Macromodels for Sensor Devices,” Proc. of EuroSimE, 2005, pp. 50-54

[18] Mähne T., Kehr K., Franke A., Hauer J., Schmidt B.: “Creating Virtual Prototypes of Complex MEMS Transducers Using Reduced-Order Modelling Methods and VHDL-AMS”, Applications of Specification and Design Languages for SoCs: Selected papers from FDL'05, 2006, pp. 135-153
[19] Gugel D., Dötzel W., Ohms T., Hauer J.: “Reduced Order Modeling in Industrial MEMS Design Processes”, Proc. of Eurosensors XX, 2006, pp. 48-55
[20] Hauck T., Schmadlak I., Mehner J.: “Stress Analysis of a Micromachined Inertial Sensor at Dynamic Load“, Proc. of ITHERM, 2008, pp. 945-948
[21] Wibbeler, J.; Mehner, J.; Vogel, F.; Bennini, F.: “Development of ANSYS/Multiphysics Modules for MEMS by CAD- FEM GmbH“, Intern. Congress on FEM Technology, Bd. 2, 2.4.6, 2001
[22] Mehner J., Dötzel W., Schauwecker B., Ostergaard D., “Reduced Order of Fluid Structural Interactions in MEMS Based on Modal Projection Techniques”, Proc. of Transducers 2003, Boston, MA, Jun. 2003, pp. 1840-1843
[23] Gugel D., Dötzel W.: “Parametric Reduced Order Modeling for Industrial MEMS Design Processes”, Proc. of Smart Systems Integration, 2007, pp. 65-72
[24] Niessner M., Iannacci J., Schrag G.: "Mechanical contact in system-level models of electrostatically actuated RF-MEMS switches: experimental analysis and modeling", Proc. of SPIE 8066, Smart Sensors, Actuators, and MEMS V, 80660Y, May 05, 2011.
[25] Mehner J., Kurth S., Billep D., Kaufmann C., Kehr K., Dötze, W.: “Simulation of Gas Damping in Microstructures with Nontrivial Geometries”, Proc. of MEMS'98, Heidelberg, Germany, 1998, pp. 172-177
[26] Turowski M., Chen Z., Przekwas A.: “Squeeze film behaviors in MEMS for large amplitude motion - 3D simulations and nonlinear circuit/behavioral models”, Proc. of IEEE/VIUF International Workshop on Behavioral Modeling and Simulation, Orlando, Oct. 1998
[27] Naumann M., Koury D., Lin D., Oi H., Miller T.F., Mehner, J.: “Characterization of sticking effects by surface micromachined test structures”, 9. Chemnitzer Fachtagung Mikromechanik & Mikroelektronik, 2009, pp. 103-107
[28] Naumann M., Mehner J., Lin D., Miller T.: “Dependency of sticking effects on environmental conditions at MEMS devices”, 10. Chemnitzer Fachtagung Mikrosystemtechnik, 2010, pp. 77-80
[29] Naumann M., Lin D., Mehner J., Miller T.: “Design and Application of Flexible Stops for MEMS Devices”, IEEE Sensors Conf, Hawaii, 2010, pp. 168-173
[30] Naumann M., Lin D., Mehner J., McNeil A., Miller, T. F.: “Design Evaluation of Shock Induced Failure Mechanisms of MEMS by Correlation of Numerical and Experimental Results”, Proc. of Transducers 2011, Beijing, China, Jun. 2011
[31] Cullinan M. A., Culpepper M. L.: "Carbon nanotubes as piezoresistive micro-electromechanical sensors: Theory and experiment", Physical Review B82, 115428, 2010